Regenerative Therapy 28 (2025) 383–393

Contents lists available at ScienceDirect

Regenerative Therapy

journal homepage: http://www.elsevier.com/locate/reth

Original Article

Fenugreek seed extract combined with acellular nerve allografts promotes peripheral nerve regeneration and neovascularization in sciatic nerve defects

Yuanyuan Han, Zhiwei Liu, Chunjie Song*

Department of Neurology, Suqian First Hospital, Suzhi Road 120, Suqian, 223800 Jiangsu Province, China

ARTICLE INFO

Article history:
Received 10 July 2024
Received in revised form
2 December 2024
Accepted 23 December 2024

Keywords:
Fenugreek seed extract
Acellular nerve allografts
Peripheral nerve injury
Nerve regeneration
Angiogenesis

ABSTRACT

Background: Acellular nerve allografts (ANAs) have been confirmed to improve the repair and reconstruction of long peripheral nerve defects. However, its efficacy is not comparable to that of autologous nerve grafts, which are used as the gold standard for treating peripheral nerve defects. Our study investigated whether fenugreek seed extract (FSE) exhibits neuroprotective potential and enhances the therapeutic outcomes of ANA repair in peripheral nerve defects.

Methods: Rat Schwann cells were treated with FSE to assess the effects of FSE on cell proliferation and their secretion function of neurotrophic factors *in vitro*. Sprague-Dawley rats with a unilateral 15-mm sciatic nerve defect were randomized into the ANA group (the 15-mm defect was replaced by an 18-mm ANA), the ANA + FSE group (the 15-mm defect was repaired with an 18-mm ANA with FSE administration for four weeks), and the Auto group (the 15-mm defect was repaired with an autologous graft). After four weeks post-surgery, various behavioral tests and electrophysiological assays were performed to evaluate the motor and sensory behavior as well as nerve conduction of rats. Then, rats were sacrificed, and the nerve grafts were collected for toluidine blue staining, RT-qPCR, immunofluorescence staining, immunohistochemical staining to evaluate nerve regeneration, neovascularization, and neuroinflammation. Their gastrocnemius was harvested for Masson's trichrome staining to examine gastrocnemius muscle recovery.

Results: FSE treatment promoted Schwann cell proliferation and its secretion of neurotrophic factors *in vitro*. Compared with ANAs alone, FSE treatment combined with ANAs enhanced axonal regeneration, upregulated S100, NF200, P0, MBP, and GAP43 expression, facilitated angiogenesis, and elevated neurotrophic factor expression in regenerating nerves of rats with sciatic nerve defects. In addition, FSE treatment promoted gastrocnemius muscle recovery, stimulated motor and sensory functional recovery and nerve conduction, and mitigated neuroinflammation in rats with sciatic nerve defects after repair with ANAs.

Conclusion: FSE treatment improves the beneficial effects of ANA repair on sciatic nerve defects.

1. Introduction

Traumatic injuries to peripheral nerves, which are ascribed to crushing, stretching, blunt or sharp forces, and various other causes, are common issues during clinical practice [1]. This type of nerve damage can result in severe loss of motor and sensory functions and even lifelong disability, placing a huge socio-economic burden on the community [2]. Nerve repair after injury is a series of complex pathological processes, and the slow process of nerve regeneration, formation of scar tissue, inhibition of the microenvironment, motor terminal organization, functional degradation, and other factors can all constrain the repair of injured nerves [3]. Small nerve defects can be restored by the nerve's repair ability, while the repair and functional reconstruction of long defective nerves is still a clinical challenge in neurosurgery, which seriously affects the health and life quality of patients [4]. Autologous nerve grafting is the gold standard approach for bridging peripheral nerve defects [5]. Nevertheless,

* Corresponding author. Suqian First Hospital, Suzhi Road 120, Suqian, 223800 Jiangsu Province, China.
E-mail addresses: 13913966899@163.com, songchunjie@stu.ahu.edu.cn (C. Song).

Peer review under responsibility of the Japanese Society for Regenerative Medicine.

https://doi.org/10.1016/j.reth.2024.12.015

several drawbacks including secondary trauma, dysfunction of donor sites, shortage of donor sources, postoperative neuromatous pain, and scarring greatly restrict the clinical application of autografts [6], which prompts researchers to look for another way to repair extensive nerve injuries.

Various alternative techniques to nerve autografts have been investigated, including allografts, biocatheters, and synthetic catheters, among which acellular nerve allografts (ANAs) seem to be the most promising [7]. Since ANAs are derived from native peripheral nerves, they can preserve the internal structure of the nerve and the active components of the extracellular matrix in a more intact manner, and at the same time remove allogeneic nerve immunogenic substances and retain a nonimmunogenic nature [8]. Currently, a variety of methods such as irradiation, lyophilization, enzymatic preparations, chemical detergent, freeze-thaw cycling, and cold preservation have been studied to prepare ANAs [9]. An increasing number of clinical and animal studies have demonstrated ANAs as ideal peripheral nerve grafts, which yield good effectiveness for the repair of peripheral nerve defects [10,11]. However, the nerve regeneration and functional repair efficiency of ANAs will attenuate as the length of the nerve graft increases, which may be due to the loss of the normal environment created by living cells to promote nerve regeneration [12]. Since ANAs still fail to keep pace with autologous nerve grafting in therapeutic outcomes, it is necessary to search for more effective methods to advance the bridging capacity of ANAs.

Fenugreek (*Trigonella foenum graecum* Linn), which belongs to the family Fabaceae, is cultivated around the world as a semiarid crop [13]. It is also recognized in South Asia and Middle East as a homology of medicine and food, whose seeds are commonly used not only as a spice in food preparation but also as traditional medicines for the treatment of gastrointestinal ailments, inflammations, high cholesterol, and diabetes [14,15]. Fenugreek seed extract (FSE) mainly includes flavonoids, nicotinic acid, alkaloids, steroidal saponins, polysaccharides, and trigonelline, which are considered to account for the positive role of FSE in health including anti-inflammatory, antibacterial, anti-oxidation, hypocholesterolemic, hypoglycemic, growth performance improvement, and immunostimulating activities [16,17]. In addition, the neuroprotective effects of FSE have been confirmed in the experimental models of several neurological diseases. For example, Moghadam et al. reported that treatment with FSE improved peripheral neuropathy and restored the function of nerve fibers in pyridoxine-induced neuropathic mice [18]. Preet et al. suggested that mixed feeding of standard pellet food and fenugreek seed powder protected the sciatic nerves against structural abnormalities in diabetic rats [19]. Prema et al. discovered that fenugreek seed powder ameliorated amyloid and tau pathology, memory deficits, inflammation, and oxidative stress in aluminum chloride-induced Alzheimer's disease rat models [20]. However, the combined use of ANAs with FSE for the treatment of peripheral nerve injury has not been investigated before.

In our research, rat models with a 15-mm sciatic nerve defect were established, on which ANA implantation was performed, followed by daily administration with FSE for 4 weeks. The effects of FSE treatment combined with ANA implantation on peripheral nerve regeneration and vascularization *in vivo* were assessed. Furthermore, we explored the influence of FSE treatment on Schwann cell proliferation and secretory function *in vitro*.

2. Materials and methods

2.1. Cell culture

Rat Schwann cells (#LM-R111; LMAI Bio, Shanghai, China) were incubated in Dulbecco's Modified Eagle Medium/F12 (#10565018; Reanta, Beijing, China) containing 10 % fetal bovine serum (#ZY140661; Zeye, Shanghai, China) and 1 % penicillin/streptomycin (#C55-SV30010; Canspec; Shanghai, China) at 37 °C in a 5 % CO_2 humidified atmosphere. The medium was renewed every 2 days, and cells were passaged every 3 days.

2.2. Cell viability assay

FSE (2 % alkaloids, 10 % fenugreek flavones, 15 % saponin, 50 % fenugreek polysaccharide) extracted by water was supplied by Hunan Geneham Pharmaceutical Co., Ltd (Changsha, China). The changes in Schwann cell viability in response to FSE treatment were detected with the aid of a Cell Counting Kit-8 (CCK-8; #CSGK10001; Chemstan, Wuhan, China). Briefly, cells were seeded (2×10^3 cells/well) into 96-well plates and allowed to adhere overnight. Subsequently, cells were treated with FSE (0, 20, 40, 60, 80, 100, 200, and 400 μg/mL) for 48 h, after which the medium was refreshed and the CCK-8 solution (10 μL/well) was added. The optical absorbance at 450 nm was measured using a microplate reader (BioTek, Winooski, VT, USA) after another 2 h incubation at 37 °C with 5 % CO_2.

2.3. Preparation of ANA

Twelve male Sprague-Dawley rats (Vital River Co. Ltd., Beijing, China) were euthanized by intraperitoneal injection of sodium pentobarbital (50 mg/kg) to prepare ANA. After sterilizing the skin in the bilateral thigh, the bilateral sciatic nerves were exposed and resected. The nerve segments were immediately immersed in phosphate-buffered saline (PBS), and cellular components were removed by using chemical detergents following the detailed procedure developed by Sondell et al. [21]. In brief, the nerves were placed in deionized distilled water and agitated for 7 h, followed by overnight washing in 3 % Triton X-100 and 24 h incubation in 4 % sodium deoxycholate. After further washing in PBS, the nerves were immersed for 12 h in Cobalt-60 for sterilization. Finally, the allografts were preserved in sterile PBS at 4 °C before being used.

2.4. Animal feeding and grouping

Twenty-four male SPF Sprague-Dawley rats aged 6 weeks and weighing 200–300 g were purchased from Vital River Co. Ltd. Animals were maintained in a temperature (25 °C)- and humidity (55 %)- controlled room, with a 12:12 h light-dark cycle and *ad libitum* access to standard laboratory food and drink. Rats were randomly assigned into the ANA group, the ANA + FSE group, and the Auto group (n = 8/group). All experimental procedures were approved by the Administration Committee of Experimental Animals of Suqian First Hospital and followed the NIH Guide for the Care and Use of Laboratory Animals.

2.5. Surgical procedures

The sciatic nerve defects model was constructed in Sprague-Dawley rats as previously described [22]. Briefly, after anesthesia by intraperitoneal administration with sodium pentobarbital (30 mg/kg), the rats were fixed in a prone position, and a 2–4 cm curved incision was made on the sterilized skins in the right thigh and buttock. Then, the sciatic nerve was exposed by bluntly dissecting the gluteal muscles. To establish the sciatic nerve defects model, 15-mm of unbranched sciatic nerves were resected with the aid of a surgical microscope. In the ANA and ANA + FSE groups, a 15-mm segment of the sciatic nerve was replaced by an 18-mm ANA. FSE (200 mg/kg) administration began 24 h after the surgery and continued for 4 consecutive weeks. The dose of FSE was determined based on the previous study [16]. FSE was diluted in

distillate water to a volume of 1 mL and given to rats daily through the intragastric route [23]. In the autograft group, a 15-mm segment of the sciatic nerve was removed, inverted, and reimplanted into the gap. The muscle and skin were closed using 6-0 and 4-0 polyamide sutures, respectively.

2.6. Functional assessment

Gait analysis, rotarod assay, and hot plate test were performed at 4 weeks post-injury to assess the motor and sensory functional recovery of the injured hindlimb of rats after sciatic nerve defects. Each rat was trained for 2 days prior to testing, with at least 2 h of rest between tests. The results of all tests were finally recorded by a research assistant blinded to the experimental grouping.

2.7. Gait analysis

The motor function of the experimental rats following sciatic nerve engraftment was analyzed using a CatWalk XT gait analysis system (Catwalk XT, Noldus Information Technology, Wageningen, Netherlands) [24]. The hindpaws of rats were inked and the rats were allowed to walk freely through a plastic tunnel lined with paper. After recording the pawprints left on the paper as the rats crossed the tunnel with a video camera, the following parameters were measured: distances between the third toe and heel (PL), first and fifth toe (TS), and second and fourth toe (ITS) of the hind paw on the side that underwent surgery (EPL, ETS, and EITS, respectively) and on the unaffected contralateral side (NPL, NTS, and NITS, respectively). Scoring for the sciatic function index (SFI) was conducted weekly post-surgery based on the formula: SFI = 109.5 (ETS-NTS)/NTS - 38.3 (EPL-NPL)/NPL + 13.3 (EITS-NITS)/NITS - 8.8. The score of SFI ranged from −100 (represented a complete loss of function) to 0 (indicated normal walking function).

2.8. Rotarod assay

An accelerating rotarod assay was performed with LE8200 equipment (Panlab, Harvard Apparatus, Holliston, MA) that consists of a rod (diameter: 30 mm) to evaluate the motor coordination and balance abilities of rats [25]. The speed (rpm) of the rotating rod (rotarod) was gradually increased, and the rats were required to walk/run in sync with the speed to balance on the rotarod. The residence time (s) of each rat on the rotating rod was measured and recorded. In each trial, the rotarod was accelerated from 4 to 40 rpm, increasing at a rate of 1 rpm in 5 min, with each successive speed maintained for about 8 s. The motor score on the day of assessment was calculated based on the average of three rotational tests with a minimum of 5 min between each test.

2.9. Hot plate test

A hind paw thermal withdrawal test was carried out using a hot-plate instrument (Muromachi Kikai, Tokyo, Japan) to estimate the sensory function recovery in rats [26]. The rats were habituated twice to the hot plate set to room temperature before performing the test. Afterwards, each rat was placed on the hot plate, which was heated at a temperature of 55 ± 0.5 °C. To avoid any tissue injury to the paw, the maximum exposure time of rats to the hot plate was set at 60 s. The reaction time (s) of all rats towards thermal heat, manifested by hind paw licking or jumping response, was defined as the withdrawal latency and recorded.

2.10. Electrophysiological evaluation

The rats were anesthetized by an intraperitoneal injection of 40 mg/kg pentobarbital 2 h after the final functional behavioral test and subjected to electrophysiological analysis to determine the neuromuscular function level after sciatic nerve graft. After exposing the sciatic nerve, stimulating electrodes (13 mm long, 0.5 mm diameter) were inserted on the proximal and distal ends of the nerve grafts. Two recording electrodes (13 mm long, 0.5 mm diameter) were inserted subcutaneously into the middle of the intrinsic foot muscle. To assess the nerve conduction strength and nerve conduction speed, the amplitude and latency of the compound muscle action potential (CMAP) were recorded and analyzed with a set of electrophysiological recorders (Axon Digidata 1550 Digitizer, Molecular Devices).

2.11. RT-qPCR

Total RNA was isolated from rat Schwann cells and rat regenerating nerves using TRIzol reagent (#AWR0091a; Abiowell, Hunan, China) following the manufacturer's protocol. The cDNA was obtained using the HyperScript RT Supermix Reagent Kit (#R202-02; NovaBio, Shanghai, China). Real-time qPCR was conducted in triplicate for each specimen using a SYBR qPCR Mix kit (#Q204-01; NovaBio) on the StepOnePlus™ platform (Applied Biosystems, Foster City, CA, USA). Primers used in our study were as follows: BDNF: F, 5′-TTCATTGAGCCCAGTTCCA-3′ and R, 5′-TTTGCTTCTTTCATGGGCG-3'; GDNF: F, 5′-GTAAGACGCTTCTCGAAGC-3′ and R, 5′-GGCATATTGGAGTCACTGG-3'; VEGF: F, 5′-AACTTCTACCCGTGCCTT-3′ and R, 5′-ACTTAGGTCAGCGTTTCC-3'; NGF: F, 5′-ATCGCTCTCCTTCACAGAG-3′ and R, 5′-CATTACGCTATGCACCTCAG-3'; CNTF: F, 5′-GACCTGACTGCTCTTATGGA-3′ and R, 5′-CCATCCACTGAGTCAAGGT-3'; and GAPDH: F, 5′-AACTCCCATTCTTCCACCT-3′ and R, 5′-TTGTCATACCAGGAAATGAGC-3'. The relative expression levels of the target genes were calculated using the $2^{-\Delta\Delta Ct}$ method and normalized to GAPDH.

2.12. Western blotting

Rat Schwann cells were harvested and lysed in RIPA buffer (#mlsw-2591; Mlbio, Shanghai, China) to prepare protein samples, whose concentrations were determined using a bicinchoninic acid protein assay kit (#ZY80815; Zeye). Samples with equal amounts of protein were electrotransferred to nitrocellulose membranes after being resolved by 10 % SDS-polyacrylamide gels. After that, 5 % non-fat milk in Tris Buffered Saline with Tween 20 (TBST) was used to block the membranes for 1 h at room temperature (RT), followed by overnight incubation at 4 °C with primary antibodies (ABclonal, Wuhan, China) including p-AKT (#AP1208; 1:1000), AKT (#A17909; 1:1000), PCNA (#A12427; 1:1000), BDNF (#A11028; 1:1000), GDNF (#A14639; 1:1000), VEGF (#A12303), NGF (#A14216; 1:1000), and GAPDH (#AC001; 1:10000) and 1 h incubation at RT with the corresponding secondary antibody (#AS014; 1:2000; ABclonal). In the end, chemiluminescence reagents (#BMU101-CN; Abbkine, Shanghai, China) were added to the membranes, which were then observed using an AI600 imaging system (GE Healthcare, USA). ImageJ software (NIH, USA) was employed for densitometry analysis, with GAPDH as an internal reference.

2.13. Toluidine blue staining

Rats were sacrificed four weeks after surgery, and the middle part of the repaired nerve segments was collected, quickly fixed for 6 h in 2.5 % glutaraldehyde, and then immersed for 2 h at 4 °C in 1 % osmium tetroxide (pH 7.3). After being serially dehydrated in increasing concentrations of ethanol, the tissues were embedded in

resin and cross-cut into 1-μm-thick sections, which were stained with toluidine blue (#AWI0473a; Abiowell) and photographed under an optical microscope (Olympus). Axonal regeneration was analyzed by calculating the axon diameter and remyelinated nerve fiber density using ImageJ software.

2.14. Immunofluorescence staining

Four weeks after surgery, the nerve grafts were harvested for immunofluorescence staining of S100, NF200, and CD31. The samples were fixed with 4 % paraformaldehyde, dehydrated with 30 % sucrose solution, and 12-μm-thick transverse or longitudinal sections of the grafted nerve were serially cut using a cryostat (Leica). The sections were then immunolabeled with primary antibodies including S100 (#A23159; 1:100; ABclonal), NF200 (#A19084; 1:100; ABclonal), CD31 (#A19014; 1:100; ABclonal), P0 (#HZK-12400; 1:100; Huzhen, Shanghai, China), MBP (#A25814; 1:100; ABclonal), and GAP43 (#A19055; 1:100; ABclonal). The next day, the appropriate second antibody conjugated with Alexa Fluor 488 (#AS053; 1:100; ABclonal) was added for 1 h at RT. Finally, the sections were imaged using an Olympus BX41 epifluorescent microscope. The density of positive immunolabelling was analyzed semi-quantitatively using ImageJ software.

2.15. Muscle evaluation

After rats were sacrificed four weeks post-surgery, the gastrocnemius was completely stripped. Their wet weight ratios were calculated by the wet weight of the injured side versus that of the normal side. Afterwards, the gastrocnemius muscle was fixed overnight in 4 % paraformaldehyde, washed, dehydrated in graded ethanol, and embedded in paraffin wax. The samples were then cross-cut into 5-μm-thick slices, which were subjected to Masson trichrome staining (#BP-DL022; Sbjbio, Nanjing, China). Photographs were obtained under a microscope and the cross-sectional area of the muscle fibers was analyzed quantitatively using ImageJ software.

2.16. Immunohistochemical staining

The paraffin-embedded sections of the grafted nerve were consecutively cross-cut into 5-μm-thick slices. After being baked for 2 h at 60 °C in a drying oven, dewaxed, hydrated, and boiled in 0.01 mol/L sodium citrate antigen repair solution (pH = 6), the slides were cooled naturally at ambient temperature, followed by incubation with 3 % hydrogen peroxide solution for 15 min to inhibit endogenous peroxidase activity and with 10 % normal goat serum for 10 min to block non-specific binding. Then, the sections were incubated overnight at 4 °C with anti-IL-6 (#A11114; 1:100; ABclonal), anti-IL-1β (#ab283818; Abcam, Shanghai, China), anti-IL-10 (#A2171; 1:100; ABclonal) primary antibodies and for 30 min at 37 °C with secondary biotinylated goat anti-rabbit IgG antibody (#ab207995; 1:500; Abcam). 3,3′-diaminobenzidine (DAB) chromogenic solution was added for color development. After being washed three times with PBS, the sections were counterstained with hematoxylin and finally sealed in neutral resin. The digital images from five fields of view were randomly selected from each section and observed under an Olympus light microscope. The mean density of the positive area was quantitatively analyzed using ImageJ software.

2.17. Statistical analysis

GraphPad Prism 8.0 software (GraphPad Software, La Jolla, CA, USA) was adopted for all statistical analyses. Two-group and multigroup comparisons were analyzed using Student's t-tests or one-way ANOVA with Tukey's *post hoc* test, respectively. The results are presented as the means ± standard deviations of triplicate experiments, and significant differences were set at $P < 0.05$.

3. Results

3.1. FSE treatment promotes the proliferation and secretory function of Schwann cells

Schwann cells, a type of glial cell in the peripheral nervous system, play a critical role in nerve regeneration and functional recovery. As shown in Fig. 1A, Schwann cell viability was gradually elevated with the increase of FSE concentration, which reached the peak after treatment with FSE at the concentration of 200 μg/mL but was reduced after treatment with a higher concentration of FSE. Accordingly, FSE (200 μg/mL) was selected for the follow-up assays. The expression of neurotrophic factors in FSE-treated Schwann cells was detected by RT-qPCR, which revealed that BDNF, GDNF, VEGF, NGF, and CNTF mRNA levels were significantly upregulated after FSE treatment (Fig. 1B–F). Consistently, the results of western blotting confirmed that FSE-treated Schwann cells exhibited higher BDNF, GDNF, VEGF, and NGF protein levels than control Schwann cells. Additionally, compared to the control group, FSE was shown to enhance PCNA (a cell proliferation marker) and p-AKT protein levels in Schwann cells (Fig. 1G and H). The above observations suggest that FSE might promote Schwann cell proliferation and secretory function through activating the AKT signaling pathway.

3.2. FSE treatment increases axonal regeneration in rats with sciatic nerve defects

Next, the rat models of sciatic nerve defects were established to explore the therapeutic effects of FSE *in vivo*. At 4 weeks postoperatively, toluidine blue staining was performed on cross-sections in the middle of the grafts to evaluate axonal regeneration in the nerve grafting area of rats (Fig. 2A). The quantitative analysis suggested that the ANA + FSE and Auto groups displayed markedly increased axon diameter and myelinated nerve fiber density compared with the ANA group (Fig. 2B and C).

3.3. FSE treatment enhances S100, NF200, P0, MBP, and GAP43 expression in regenerating nerves

The nerve grafts were sectioned longitudinally and subjected to immunofluorescence staining to detect the expression of S100 (myelinated fiber). As demonstrated by the staining results and intensity quantification of S100 labeling, the ANA + FSE and Auto groups presented remarkably higher peripheral myelin levels in the sectioned nerve tissues from the Auto and ANA + FSE groups than in those from the ANA group, and S100 expression was significantly greater in the Auto group versus the ANA + FSE group (Fig. 3A and B). Furthermore, NF200 (the myelinated axon marker), P0 (the major structural protein of peripheral myelin), MBP (the remyelination marker), and GAP43 (the axonal membrane protein) expression in the cross-sections of the nerve grafts was examined. The immunofluorescence staining revealed that NF200, P0, MBP, and GAP43 expression was prominently upregulated in the ANA + FSE and Auto groups compared with the ANA group, with higher NF200, P0, MBP, and GAP43 expression in the Auto group than in the ANA + FSE group (Fig. 3C–J).

3.4. FSE treatment facilitates angiogenesis in regenerating nerves

To assess the influence of FSE on the angiogenesis in the regenerated nerve, we performed immunofluorescence staining of

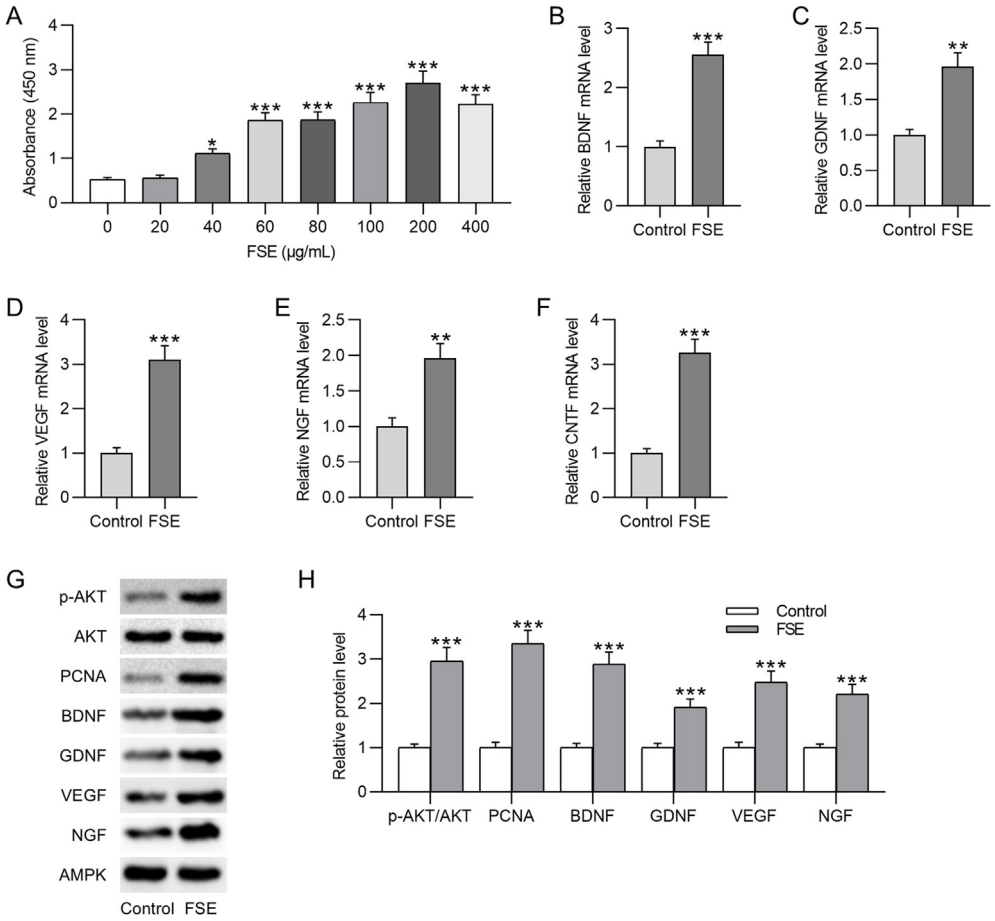

Fig. 1. FSE treatment promotes the proliferation and secretory function of Schwann cells. (A) Assessment of Schwann cell viability after 48 h treatment with FSE (0, 20, 40, 60, 80, 100, 200, and 400 μg/mL) by CCK-8 assay. (B–F) Analysis of BDNF, GDNF, VEGF, NGF, and CNTF mRNA levels in Schwann cells after treatment with or without FSE (200 μg/mL) by RT-qPCR. (G–H) Measurement of p-AKT, AKT, PCNA, BDNF, GDNF, VEGF, and NGF protein levels in control and FSE-treated Schwann cells by western blotting. *p < 0.05, **p < 0.01, ***p < 0.001.

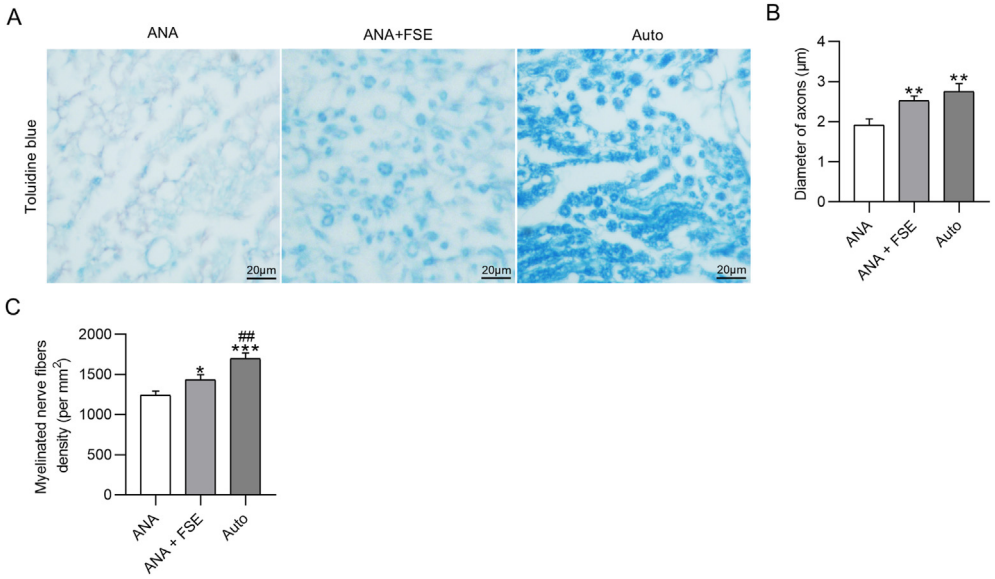

Fig. 2. FSE treatment increases axonal regeneration in rats with sciatic nerve defects. (A) Representative toluidine blue staining images showing axonal regeneration in the nerve grafting area of rats four weeks post-surgery. (B–C) Quantification of the axon diameter and myelinated nerve fiber density in each group. n = 8. *p < 0.05, **p < 0.01, ***p < 0.001 versus ANA; ##p < 0.01 versus ANA + FSE.

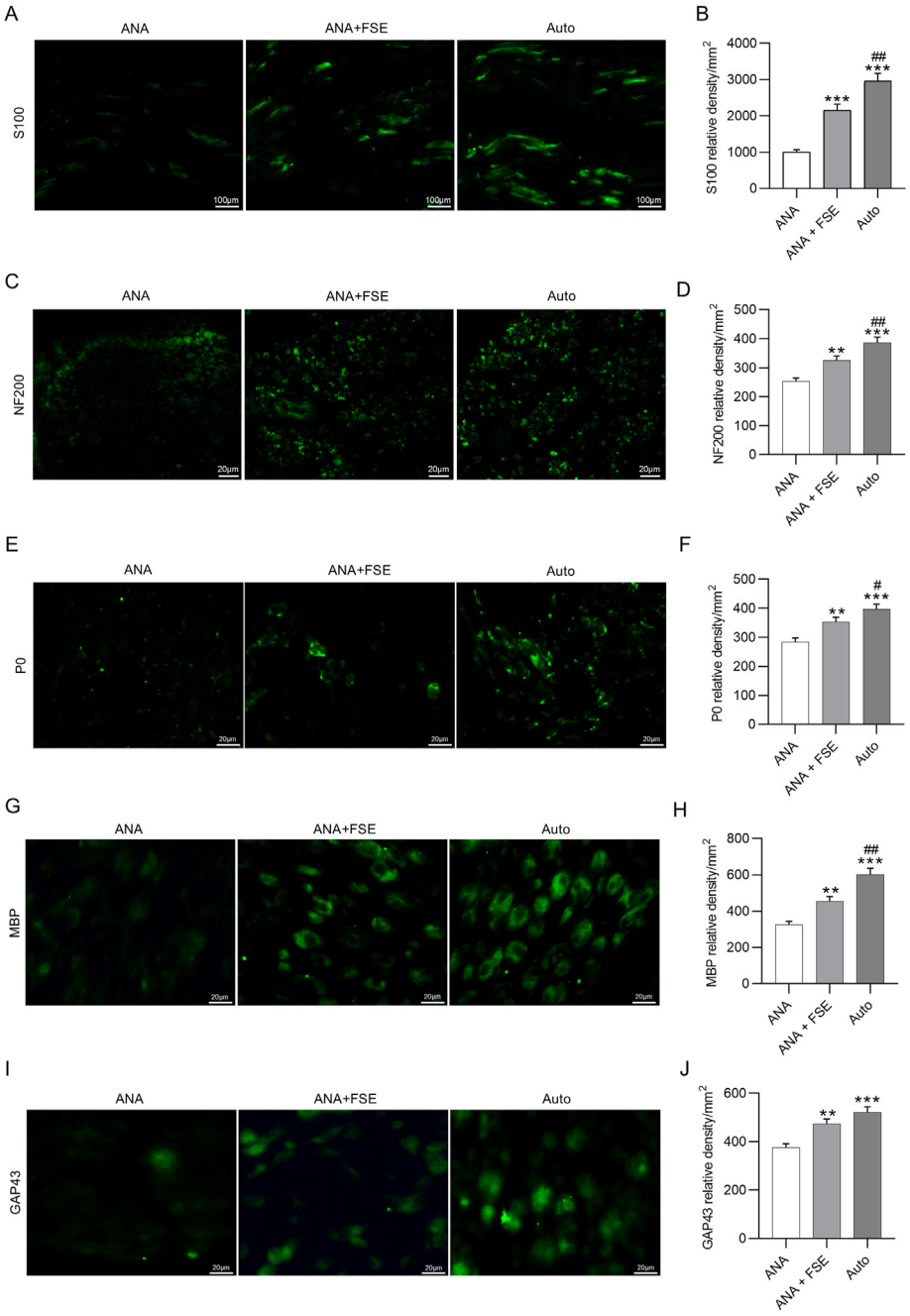

Fig. 3. FSE treatment enhances S100, NF200, P0, MBP, and GAP43 expression in regenerating nerves. (A–B) Representative immunofluorescence staining images showing S100 expression in the longitudinal sections of the nerve grafts and the quantification analysis of S100 staining density. Scale bar: 100 μm. (C–D) Representative immunofluorescence staining images showing NF200 expression in the cross-sections of the nerve grafts and the quantification analysis of NF200 staining density. Scale bar: 20 μm. (E–F) Representative immunofluorescence staining images showing P0 expression in the cross-sections of the nerve grafts and the quantification analysis of P0 staining density. Scale bar: 20 μm. (G–H) Representative immunofluorescence staining images showing MBP expression in the cross-sections of the nerve grafts and the quantification analysis of MBP staining density. Scale bar: 20 μm. (I–J) Representative immunofluorescence staining images showing GAP43 expression in the cross-sections of the nerve grafts and the quantification analysis of GAP43 staining density. Scale bar: 20 μm. n = 8. **p < 0.01, ***p < 0.001 versus ANA; #p < 0.05, ##p < 0.01 versus ANA + FSE.

the microvessels. As observed in Fig. 4A, the ANA + FSE and Auto groups showed markedly more CD31-stained (green) vascular endothelial cells than the ANA group, and the green staining in the Auto groups was more obvious than in the ANA + FSE group. The quantification results also indicated that the microvessel density was superior in the ANA + FSE and Auto groups compared with the ANA group (Fig. 4B).

3.5. FSE treatment stimulates the secretion of neurotrophic factors in rats with sciatic nerve defects

Neurotrophic factors play a crucial role in the process of nerve regeneration. RT-qPCR analysis was conducted to determine the expression of several key neurotrophic factors in rat models of sciatic nerve defects after FSE treatment. The results manifested that BDNF, GDNF, VEGF, NGF, and CNTF mRNA levels were considerably

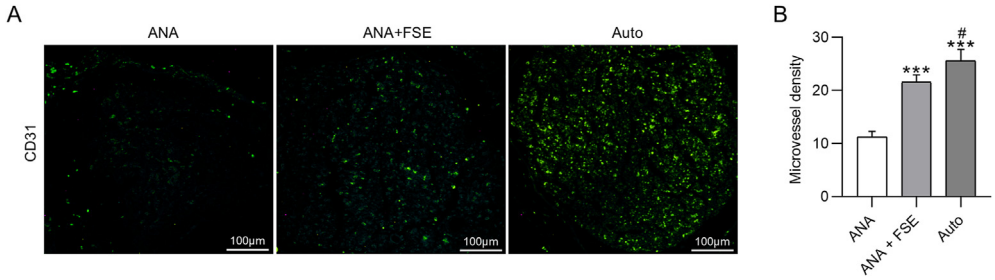

Fig. 4. FSE treatment facilitates angiogenesis in regenerating nerves. (A) Representative microvessel immunofluorescence staining images showing CD31-stained (green) vascular endothelial cells. Scale bar: 100 μm. (B) Quantitative analysis of microvessel density (per cross-section). n = 8. ***p < 0.001 versus ANA; #p < 0.05 versus ANA + FSE.

higher in regenerating nerves obtained from the ANA + FSE and Auto groups than in those from the ANA group (Fig. 5A–E).

3.6. FSE treatment promotes gastrocnemius muscle recovery in rats with sciatic nerve defects

At 4 weeks after the operation, the gastrocnemius muscles from both sides were harvested and weighed. We discovered obvious atrophy in the injured side of gastrocnemius muscles compared with the normal side in the ANA group. Nevertheless, no significant difference in muscle volume between the normal and injured side was observed in the ANA + FSE and Auto groups (Fig. 6A). The wet weight ratio was notably elevated in the ANA + FSE and Auto groups compared with the ANA group, with an even higher wet weight ratio in the Auto group than in the ANA + FSE group (Fig. 6B). Through Masson's trichrome staining, it was observed that blue-stained collagen fibers were more prominent in the ANA group (Fig. 6C). The mean cross-sectional area of the gastrocnemius muscle was evidently greater in the ANA + FSE and Auto groups than in the ANA group. The ANA + FSE and Auto groups exhibited no significant difference in the cross-sectional area (Fig. 6D).

3.7. FSE treatment enhances functional recovery in rats with sciatic nerve defects

The SFI is widely used as an important parameter to measure reflexive motor function following sciatic nerve injury. The results showed that the SFI value was markedly higher in the ANA + FSE and Auto groups than in the ANA group (Fig. 7A). A rotarod test was conducted to examine motor coordination and balance, which showed that the rats in the ANA + FSE and Auto groups remained on the rotating rod longer than those in the ANA group (Fig. 7B). Moreover, the hot plate test was employed to assess sensory functional recovery, in which longer latency represented a sluggish sensory function in the tested foot. As expected, the ANA + FSE and Auto groups exhibited considerably shorter latency than the ANA group (Fig. 7C). The improved nerve regeneration was also accompanied by nerve conduction electrophysiological improvements. The results revealed that the amplitude of the CMAP was increased while the latency of the CMAP was decreased in the ANA + FSE and Auto groups compared with the ANA group (Fig. 7D and E).

3.8. FSE treatment mitigates neuroinflammation in rats with sciatic nerve defects

Finally, whether FSE treatment combined with ANA implantation can alleviate inflammatory response in the nerve grafting area was estimated. The levels of pro-inflammatory and anti-inflammatory cytokines in the grafted nerve were observed through immunohistochemical staining. The data depicted that IL-6 and IL-1β expression was prominently weakened and IL-10 expression was enhanced in the ANA + FSE and Auto groups, compared with the ANA group (Fig. 8A–D).

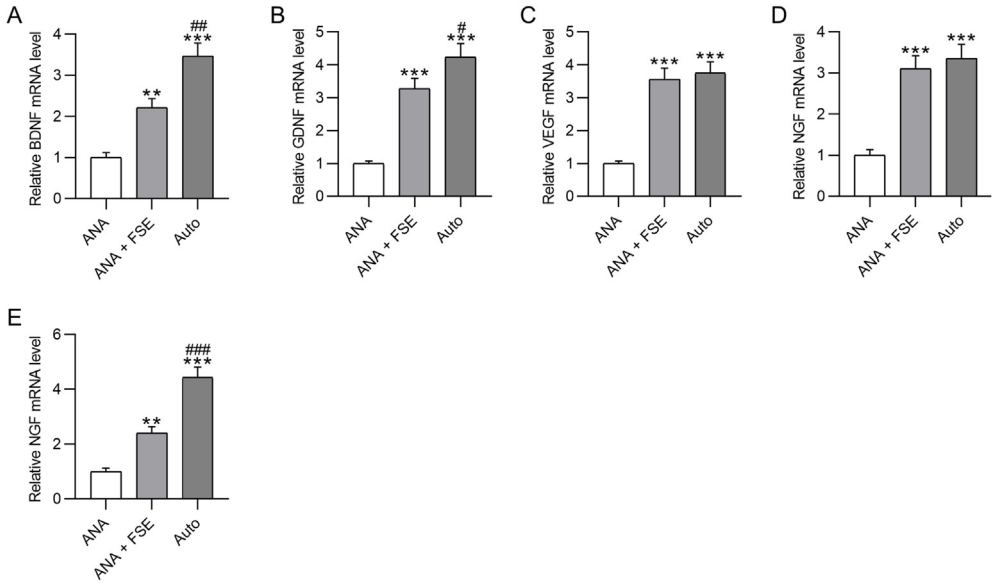

Fig. 5. FSE treatment promotes the secretion of neurotrophic factors in rats with sciatic nerve defects. (A–E) Examination of BDNF, GDNF, VEGF, NGF, and CNTF mRNA levels in regenerating nerves by RT-qPCR. n = 8. **p < 0.01, ***p < 0.001 versus ANA; #p < 0.05, ##p < 0.01, ###p < 0.001 versus ANA + FSE.

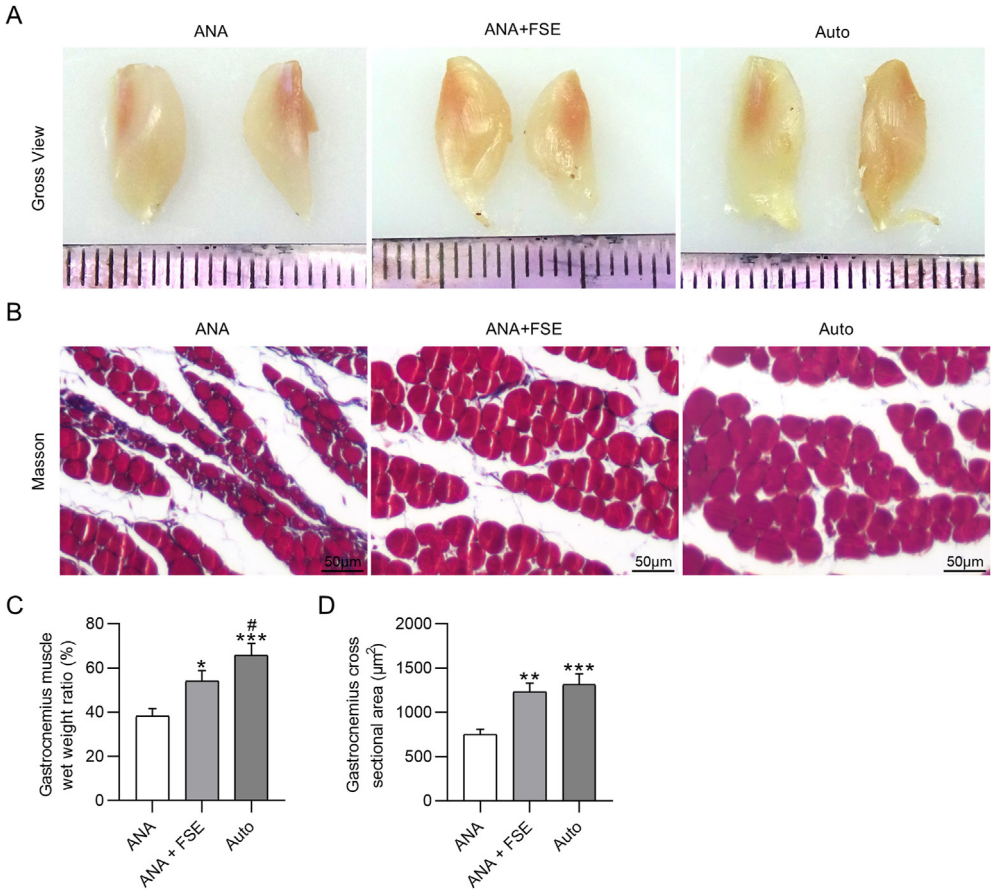

Fig. 6. FSE treatment promotes gastrocnemius muscle recovery in rats with sciatic nerve defects. (A) Representative gross views of gastrocnemius muscles in the normal (left) and injured side (right). (B) Representative Masson's trichrome staining showing blue-stained collagen fibers. Scale bar: 50 μm. (C) Quantification of gastrocnemius muscle wet weight ratio (injured/normal side). (D) Quantification of the mean gastrocnemius cross-sectional area. n = 8. *p < 0.05, **p < 0.01, ***p < 0.001 versus ANA; #p < 0.05 versus ANA + FSE.

4. Discussion

This is the first research investigating the effects of FSE administration on ANA bridging in animal models of long-gap sciatic nerve defects. Through *in vitro* examination, we discovered that FSE stimulated Schwann cell proliferation and secretory function. Besides, FSE effectively improved the bridging effect of ANAs in sciatic nerve injury rat models, as evidenced by the better effects of FSE combined with ANAs than ANAs alone on promoting nerve regeneration and neovascularization as well as ameliorating muscular atrophy, functional recovery, and neuroinflammation.

Peripheral nerve injury mainly refers to the peripheral nerve trunk or its branches by external direct or indirect force and damage. The most common clinical causes are mechanical injuries such as sharp cuts, nerve compression injuries, and pulling injuries. It can cause sensory and motor dysfunction, and may lead to life-long disability without timely, effective, and correct repair treatment [27]. In recent years, neurosurgery has been focused on searching for effective repair and reconstruction methods. At present, surgery, gene therapy, tissue engineering, and nerve grafts (autografts, allografts, and xenografts) have been identified as desirable treatments for peripheral nerve deficits [28]. Although autologous nerve grafting is regarded as the classic treatment method of choice for repairing peripheral nerve defects, the secondary motor and sensory deficits at the donor sites as well as the scarcity of resources largely limit its clinical application [29]. As an important alternative strategy, several nerve conduits have made significant progress in the repair of large and segmental nerve injuries and defects, among which ANAs have the most potential. Such a technique chemically removes most of the immunogens (e.g., Schwann cells) and preserves only the reticular structure of the nerve, thus greatly neutralizing the immune rejection [30]. Furthermore, a distinct advantage of the ANA approach over other synthetic nerve conduits is that the nerve length can be readily adjusted as needed [31]. However, ANAs are not comparable to autologous nerve grafts in terms of therapeutic efficacy. Hence, the exploration of adjunctive measures to enhance the role of ANAs in bridging peripheral nerve defects is under great urgency. Previously, the beneficial role of FSE in ameliorating peripheral neuropathy in animal models was demonstrated [32]. In our study, rats with sciatic nerve defects were further administrated with FSE after repair with ANAs, and the findings indicated that FSE combined with ANAs better promoted axon regeneration and remyelination compared with ANAs alone, as evidenced by increased axon number and diameter, myelinated nerve fiber density, and myelin sheath thickness, decreased axon-to-fiber diameter ratio (G-ratio) as well as elevated S100, NF200, P0, MBP, and GAP43 expression in regenerating nerves. Additionally, we further validated that FSE combined with ANAs exhibited better effects in alleviating muscle atrophy, promoting functional recovery, and mitigating neuroinflammation than ANAs alone.

Glial cells in the peripheral nervous system are known as Schwann cells, which are distributed along the protrusions of neurons and wrapped around the outer axon [33]. Among them,

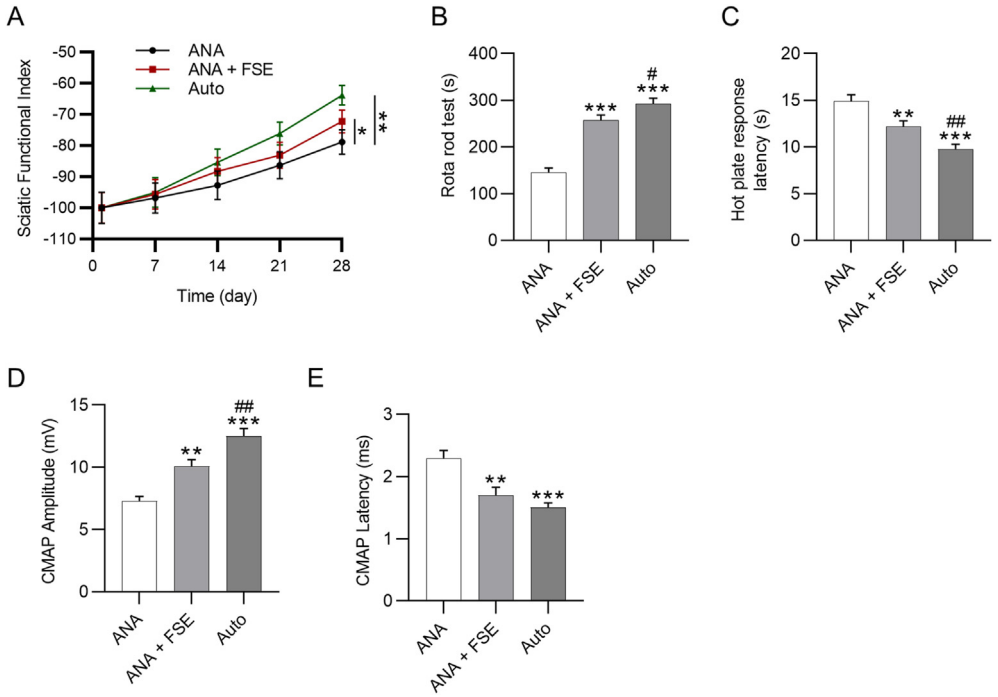

Fig. 7. FSE treatment enhances functional recovery in rats with sciatic nerve defects. (A) Scoring of the sciatic function index (SFI) based on gait analysis. (B) The time of rats remaining on the rotating rod according to rotarod assay results. (C) The withdrawal latency from a hot plate based on hot plate test results. (D–E) Quantification analysis of compound muscle action potential (CMAP) amplitude and latency of three groups. n = 8. *p < 0.05, **p < 0.01, ***p < 0.001 versus ANA; #p < 0.05, ##p < 0.01 versus ANA + FSE.

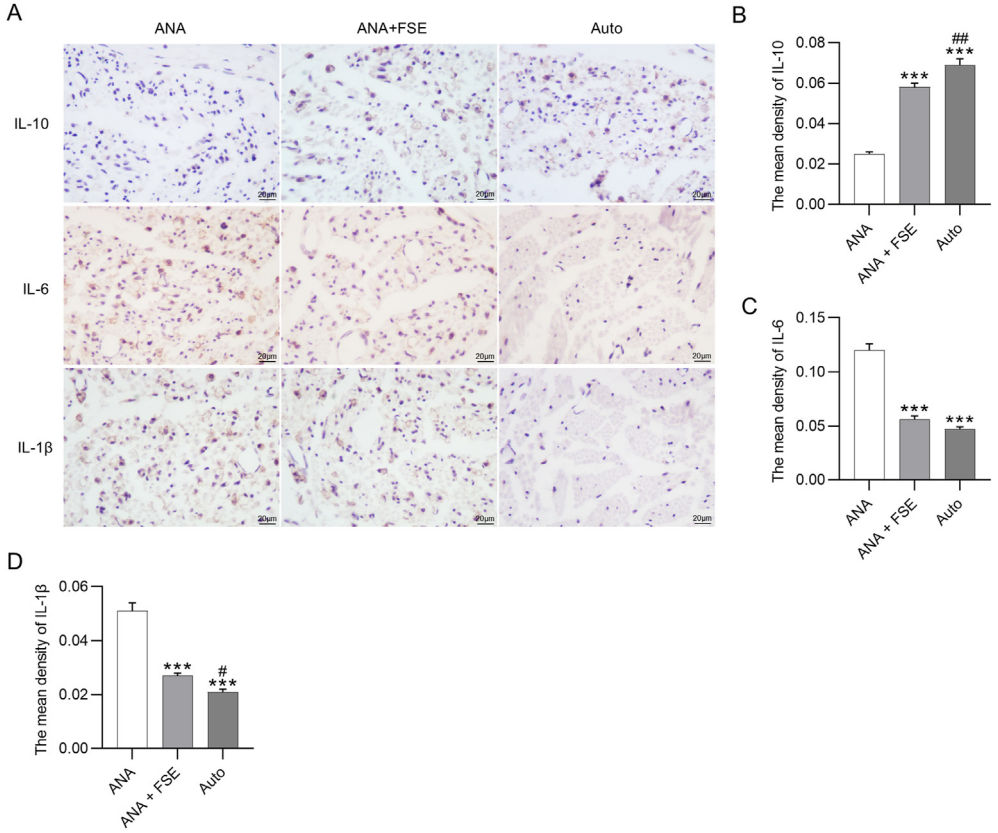

Fig. 8. FSE treatment mitigates neuroinflammation in rats with sciatic nerve defects. (A) Representative immunohistochemical staining images showing IL-6, IL-1β, and IL-10 expression in the cross-sections of the nerve grafts. Scale bar: 20 μm. (B–D) Quantification of IL-6-, IL-1β-, and IL-10-positive areas in each group. n = 8. ***p < 0.001 versus ANA; #p < 0.05, ##p < 0.05 versus ANA + FSE.

myelin-forming Schwann cells, which encapsulate large-calibre axons, form myelin sheaths outside the axons, while non-myelin-forming Schwann cells wrap around small-calibre axons to produce unmyelinated axons [34]. During the first few days after peripheral nerve injury, Wallerian degeneration takes place in the distal axonal stump. The whole process of Wallerian degeneration includes degeneration of the axons, shedding, and degradation of the myelin sheath, and proliferation of Schwann cells within their basal lamina tubes [35]. Wallerian degeneration produces residual axons and myelin fragments that inhibit nerve growth, which need to be removed before nerve regeneration [36]. In injured nerves, Schwann cells undergo adaptive cellular reprogramming to become repair-competent cells that facilitate the disassembly of damaged axons. Subsequently, Schwann cells coordinate the removal of myelin debris through myelin autophagy, phagocytosis, and attraction of macrophages, promote axonal regeneration, and eventually rebuild myelin [37]. Schwann cells are highly plastic and are vital for the process of axonal regeneration after peripheral nerve injury or lesions [38]. Importantly, they serve as a crucial source of neurotrophic factors, such as BDNF, GDNF, NGF, and CNTF. Neurotrophic factors promote neurite growth, differentiation, survival and protrusion regeneration by binding to receptors on neurons, thereby playing a key role in the development of the nervous system and its repair after injury [39]. These factors exert trophic effects on the axons regenerating from the proximal stump after diffusing across the injury area from the distal stump [40]. Herein, our data revealed that FSE treatment enhanced cell proliferation as well as upregulated BDNF, GDNF, NGF, and CNTF levels in Schwann cells, suggesting that FSE facilitated the secretion of neurotrophic factors by Schwann cells.

Blood supply is very important for the regeneration and repair of injured peripheral nerves [41]. A rich blood supply not only enables the faster removal of degenerated and disintegrated axons and myelin debris in the injured nerve to reduce secondary inflammatory damage, but also provides nutrients for the Schwann cells and enhances their biological functions, which facilitates the regeneration of axons in the injured nerve, accelerates the myelin reforming of regenerated axons, and promotes the growth and maturation of the regenerated nerve fibers and the recovery of the nerve function [42,43]. Adequate blood supply is especially critical in the repair of long-distance and large-diameter nerve defects [44]. After peripheral nerve injury, the timing of angiogenesis precedes the migration of Schwann cells and the extension of axons [42]. Re-vascularization of nerve grafts provides necessary nutrient and material exchange channels and guides myelin regeneration for structural reconstruction and functional recovery [45]. In addition, trophic factors secreted by new blood vessels, such as vascular endothelial growth factor (VEGF), GDNF, and NGF, contribute to guiding axonal growth [46]. VEGF is a key regulator of angiogenesis, which promotes the division and migration of endothelial cells and induces angiogenesis [47]. Wongtrakul et al. discovered that neurovascular density and neural blood flow were significantly increased after short-term local application of VEGF in rabbit models of sciatic nerve defects [48]. Macrophages induce the generation of polarized blood vessels by secreting VEGF after murine sciatic nerve injury, suggesting that blood vessels can also serve as a scaffold for the crawling migration of Schwann cells and guide the growth of axonal myelin [49]. Previously, Lodra et al. reported that FSE administration markedly increased tissue blood vessels and VEGF expression in the alveolar bone tissues of ovariectomized rat models [50], indicating its angiogenesis-promoting effects. Herein, *in vitro* results showed that treatment with FSE enhanced VEGF expression in Schwann cells. Furthermore, microvessel immunofluorescence staining in the regenerated nerve of rats showed that the numbers of CD31-stained (green) vascular endothelial cells were elevated after FSE administration. Taken together, FSE promoted neovascularization after peripheral nerve injury.

To be honest, there exist several limitations in this study. First, even though the positive effects of FSE treatment on Schwann cell proliferation and neurotrophic factor secretion *in vitro* as well as on axon regeneration and angiogenesis in rat models of sciatic nerve defects were confirmed in our study, the complicated mechanism through which FSE exhibits beneficial effects on peripheral nerve regeneration has not been explored, which is a pivotal direction for future research. Second, different sexes of rats show differences in immune cell responses, vulnerability to ischemic injury, as well as cerebral vascular regulation and metabolism. Although single-sex rats were used in investigating peripheral nerve defects in most previous studies, the fact that all rats included in our study were male may introduce some experimental bias.

Collectively, ANA repair combined with FSE treatment shows superior effects than ANA repair alone, and equal effects on peripheral nerve regeneration and vascularization compared with repair with the autologous grafts. These observations imply that incorporating FSE in ANA repair may be a promising therapeutic strategy for peripheral nerve injury in the clinic.

Data availability statement

The datasets used or analyzed during the current study are available from the corresponding author on reasonable request.

Authors' contributions

Yuanyuan Han was the main designer of this study. Yuanyuan Han, Zhiwei Liu, and Chunjie Song performed the experiments and analyzed the data. Yuanyuan Han and Chunjie Song drafted the manuscript. All authors read and approved the final manuscript.

Funding

This study is Supported by Suqian Sci and Tech Programme (Granted NO KY202204).

Declaration of competing interest

The authors declare that they have no competing interests.

Acknowledgement

The authors appreciate all the participants providing supports for this study.

References

[1] Lopes B, Sousa P, Alvites R, Branquinho M, Sousa AC, Mendonça C, et al. Peripheral nerve injury treatments and advances: one health perspective. Int J Mol Sci 2022;23(2).
[2] Lin J, Shi J, Min X, Chen S, Zhao Y, Zhang Y, et al. The GDF11 promotes nerve regeneration after sciatic nerve injury in adult rats by promoting axon growth and inhibiting neuronal apoptosis. Front Bioeng Biotechnol 2021;9:803052.
[3] Burnett MG, Zager EL. Pathophysiology of peripheral nerve injury: a brief review. Neurosurg Focus 2004;16(5):E1.
[4] Grinsell D, Keating CP. Peripheral nerve reconstruction after injury: a review of clinical and experimental therapies. BioMed Res Int 2014;2014:698256.
[5] Yi S, Zhang Y, Gu X, Huang L, Zhang K, Qian T, et al. Application of stem cells in peripheral nerve regeneration. Burns Trauma 2020;8:tkaa002.
[6] Heinzel JC, Quyen Nguyen M, Kefalianakis L, Prahm C, Daigeler A, Hercher D, et al. A systematic review and meta-analysis of studies comparing muscle-in-vein conduits with autologous nerve grafts for nerve reconstruction. Sci Rep 2021;11(1):11691.
[7] Safa B, Buncke G. Autograft substitutes: conduits and processed nerve allografts. Hand Clin 2016;32(2):127–40.

[8] Moore AM, MacEwan M, Santosa KB, Chenard KE, Ray WZ, Hunter DA, et al. Acellular nerve allografts in peripheral nerve regeneration: a comparative study. Muscle Nerve 2011;44(2):221–34.
[9] Broeren BO, Hundepool CA, Kumas AH, Duraku LS, Walbeehm ET, Hooijmans CR, et al. The effectiveness of acellular nerve allografts compared to autografts in animal models: a systematic review and meta-analysis. PLoS One 2024;19(1):e0279324.
[10] Cerqueira SR, Lee YS, Cornelison RC, Mertz MW, Wachs RA, Schmidt CE, et al. Decellularized peripheral nerve supports Schwann cell transplants and axon growth following spinal cord injury. Biomaterials 2018;177:176–85.
[11] Zhu S, Liu J, Zheng C, Gu L, Zhu Q, Xiang J, et al. Analysis of human acellular nerve allograft reconstruction of 64 injured nerves in the hand and upper extremity: a 3 year follow-up study. J Tissue Eng Regen Med 2017;11(8):2314–22.
[12] Walsh S, Biernaskie J, Kemp SW, Midha R. Supplementation of acellular nerve grafts with skin derived precursor cells promotes peripheral nerve regeneration. Neuroscience 2009;164(3):1097–107.
[13] Nagulapalli Venkata KC, Swaroop A, Bagchi D, Bishayee A. A small plant with big benefits: fenugreek (Trigonella foenum-graecum Linn.) for disease prevention and health promotion. Mol Nutr Food Res 2017;61(6).
[14] Baquer NZ, Kumar P, Taha A, Kale RK, Cowsik SM. Metabolic and molecular action of Trigonella foenum-graecum (fenugreek) and trace metals in experimental diabetic tissues. J Biosci 2011;36(2):383–96.
[15] Belguith-Hadriche O, Bouaziz M, Jamoussi K, El Feki A, Sayadi S. Lipid-lowering and antioxidant effects of an ethyl acetate extract of fenugreek seeds in high-cholesterol-fed rats. J Agric Food Chem 2010;58(4):2116–22.
[16] Hamza AA, Elwy HM, Badawi AM. Fenugreek seed extract attenuates cisplatin-induced testicular damage in Wistar rats. Andrologia 2016;48(2):211–21.
[17] Yang L, Chen L, Zheng K, Ma YJ, He RX, Arowolo MA, et al. Effects of fenugreek seed extracts on growth performance and intestinal health of broilers. Poultry Sci 2022;101(7):101939.
[18] Moghadam FH, Vakili-Zarch B, Shafiee M, Mirjalili A. Fenugreek seed extract treats peripheral neuropathy in pyridoxine induced neuropathic mice. Excli j 2013;12:282–90.
[19] Preet A, Gupta BL, Siddiqui MR, Yadava PK. Restoration of ultrastructural and biochemical changes in alloxan-induced diabetic rat sciatic nerve on treatment with Na3VO4 and Trigonella–a promising antidiabetic agent. Mol Cell Biochem 2005;278(1–2):21–31.
[20] Prema A, Justin Thenmozhi A, Manivasagam T, Mohamed Essa M. Fenugreek seed powder attenuated aluminum chloride-induced tau pathology, oxidative stress, and inflammation in a rat model of alzheimer's disease. J Alzheimers Dis 2017;60(s1):S209–20.
[21] Sondell M, Lundborg G, Kanje M. Regeneration of the rat sciatic nerve into allografts made acellular through chemical extraction. Brain Res 1998;795(1–2):44–54.
[22] Zuo J, Wu Y, Xiang R, Dai Z. ω-3 polyunsaturated fatty acids facilitate the repair of peripheral nerve defects with chemically extracted acellular allograft in rats. BioMed Res Int 2021;2021:2504276.
[23] Folwarczna J, Zych M, Nowińska B, Pytlik M. Effects of fenugreek (Trigonella foenum-graecum L.) seed on bone mechanical properties in rats. Eur Rev Med Pharmacol Sci 2014;18(13):1937–47.
[24] Wang Z, Yang X, Zhang W, Zhang P. Tanshinone IIA attenuates nerve structural and functional damage induced by nerve crush injury in rats. PLoS One 2018;13(8):e0202532.
[25] Singh S, Jamwal S, Kumar P. Neuroprotective potential of Quercetin in combination with piperine against 1-methyl-4-phenyl-1,2,3,6-tetrahydropyridine-induced neurotoxicity. Neural Regen Res 2017;12(7):1137–44.
[26] Ibrahim MA, Abdelzaher WY, Rofaeil RR. Efficacy and safety of combined low doses of either diclofenac or celecoxib with gabapentin versus their single high dose in treatment of neuropathic pain in rats. Biomed Pharmacother 2018;100:267–74.
[27] Hussain G, Wang J, Rasul A, Anwar H, Qasim M, Zafar S, et al. Current status of therapeutic approaches against peripheral nerve injuries: a detailed story from injury to recovery. Int J Biol Sci 2020;16(1):116–34.
[28] Kornfeld T, Vogt PM, Radtke C. Nerve grafting for peripheral nerve injuries with extended defect sizes. Wien Med Wochenschr 2019;169(9–10):240–51.
[29] Yu T, Wen L, He J, Xu Y, Li T, Wang W, et al. Fabrication and evaluation of an optimized acellular nerve allograft with multiple axial channels. Acta Biomater 2020;115:235–49.
[30] Isaacs J, Browne T. Overcoming short gaps in peripheral nerve repair: conduits and human acellular nerve allograft. Hand (N Y) 2014;9(2):131–7.
[31] Pereira C, Lazar SV, Wang A. Bioengineering approaches for nerve graft revascularization: current concepts and future directions. WIREs Mech Dis 2023;15(4):e1609.
[32] Morani AS, Bodhankar SL, Mohan V, Thakurdesai PA. Ameliorative effects of standardized extract from Trigonella foenum-graecum L. seeds on painful peripheral neuropathy in rats. Asian Pac J Tropical Med 2012;5(5):385–90.
[33] Nocera G, Jacob C. Mechanisms of Schwann cell plasticity involved in peripheral nerve repair after injury. Cell Mol Life Sci 2020;77(20):3977–89.
[34] Bosch-Queralt M, Fledrich R, Stassart RM. Schwann cell functions in peripheral nerve development and repair. Neurobiol Dis 2023;176:105952.
[35] Cai M, Shao J, Yung B, Wang Y, Gao NN, Xu X, et al. Baculoviral inhibitor of apoptosis protein repeat-containing protein 3 delays early Wallerian degeneration after sciatic nerve injury. Neural Regen Res 2022;17(4):845–53.
[36] Roberts SL, Dun XP, Dee G, Gray B, Mindos T, Parkinson DB. The role of p38alpha in Schwann cells in regulating peripheral nerve myelination and repair. J Neurochem 2017;141(1):37–47.
[37] Wang L, Sanford MT, Xin Z, Lin G. Role of Schwann cells in the regeneration of penile and peripheral nerves. Asian J Androl 2015;17(5):776–82.
[38] Choi SJ, Park SY, Shin YH, Heo SH, Kim KH, Lee HI, et al. Mesenchymal stem cells derived from wharton's jelly can differentiate into Schwann cell-like cells and promote peripheral nerve regeneration in acellular nerve grafts. Tissue Eng Regen Med 2021;18(3):467–78.
[39] Hoyng SA, De Winter F, Gnavi S, de Boer R, Boon LI, Korvers LM, et al. A comparative morphological, electrophysiological and functional analysis of axon regeneration through peripheral nerve autografts genetically modified to overexpress BDNF, CNTF, GDNF, NGF, NT3 or VEGF. Exp Neurol 2014;261:578–93.
[40] Terenghi G. Peripheral nerve regeneration and neurotrophic factors. J Anat 1999;194(Pt 1):1–14. Pt 1.
[41] Muangsanit P, Shipley RJ, Phillips JB. Vascularization strategies for peripheral nerve tissue engineering. Anat Rec 2018;301(10):1657–67.
[42] Caillaud M, Richard L, Vallat JM, Desmoulière A. Peripheral nerve regeneration and intraneural revascularization. Neural Regen Res 2019;14(1):24–33.
[43] Wariyar SS, Brown AD, Tian T, Pottorf TS. Angiogenesis is critical for the exercise-mediated enhancement of axon regeneration following peripheral nerve injury. Exp Neurol 2022;353:114029.
[44] Chen WH, Mao CQ, Zhuo LL, Ong JL. Beta-nerve growth factor promotes neurogenesis and angiogenesis during the repair of bone defects. Neural Regen Res 2015;10(7):1159–65.
[45] Saffari TM, Bedar M, Hundepool CA, Bishop AT. The role of vascularization in nerve regeneration of nerve graft. Neural Regen Res 2020;15(9):1573–9.
[46] Hatakeyama M, Ninomiya I, Kanazawa M. Angiogenesis and neuronal remodeling after ischemic stroke. Neural Regen Res 2020;15(1):16–9.
[47] Ballmer-Hofer K. Vascular endothelial growth factor, from basic research to clinical applications. Int J Mol Sci 2018;19(12).
[48] Wongtrakul S, Bishop AT, Friedrich PF. Vascular endothelial growth factor promotion of neoangiogenesis in conventional nerve grafts. J Hand Surg Am 2002;27(2):277–85.
[49] Cattin AL, Burden JJ, Van Emmenis L, Mackenzie FE, Hoving JJ, Garcia Calavia N, et al. Macrophage-induced blood vessels guide Schwann cell-mediated regeneration of peripheral nerves. Cell 2015;162(5):1127–39.
[50] Lodra EH, Effendi MC, Pematasari N, Dradjat RS. *Fenugreek Seed Ethanolic Extract Improves Alveolar Bone Parameters by Attenuating Inflammation in Ovariectomized Rats*. J Inflamm Res 2023;**16**:4933–40.